Neurotoxicology and Teratology 75 (2019) 106821

Contents lists available at ScienceDirect

Neurotoxicology and Teratology

journal homepage: www.elsevier.com/locate/neutera

ROS-mediated JNK pathway critically contributes to PFOS-triggered apoptosis in SH-SY5Y cells

Pingping Sun[a,b], Lingqi Gu[c], Jiashan Luo[b], Yi Qin[b], Lingli Sun[d], Shengyang Jiang[b,*]

[a] Department of Clinical Biobank, Affiliated Hospital of Nantong University, Nantong 226001, Jiangsu, People's Republic of China
[b] Department of Occupational Medicine and Environmental Toxicology, School of Public Health, Nantong University, Nantong 226001, Jiangsu, People's Republic of China
[c] Department of Pharmacy, Nantong Municipal Maternal and Child Health Hospital, Nantong, 226010, Jiangsu, People's Republic of China
[d] Department of Nutrition and Food Hygiene, School of Public Health, Nantong University, Nantong 226001, Jiangsu, People's Republic of China

ARTICLE INFO

Keywords:
Perfluorooctanesulfonate (PFOS)
JNK
ROS
Apoptosis
Neurotoxicity

ABSTRACT

Recent studies have indicated that perfluorooctane sulfonate (PFOS) and its derivatives can lead to neurotoxicity. In the present study, we showed that PFOS may trigger neuronal apoptosis through a c-Jun N-terminal kinase (JNK)-related mechanism. We revealed that c-Jun N-terminal kinase (JNK) was robustly activated in PFOS-exposed neuronal cells. The doses of PFOS that initiates JNK activation coincides with that inducing neuronal apoptosis, as confirmed by western blot and Annexin V-PE/7-AAD analyses. In addition, we found that reactive oxidative species (ROS) accumulation plays a casual role in PFOS-initiated JNK activation, as treatment with ROS scavenger *N*-acetyl-L-cysteine (NAC) abrogated PFOS-induced mitochondrial and nuclear translocation of phosphorylated JNK (p-JNK). In keeping with this notion, the expression of JNK downstream pro-apoptotic target Bim was increased following PFOS exposure in JNK- and ROS-dependent manners. Finally, Annexin V-PE/7-AAD analysis uncovered that treatment with NAC or SP600125 could significantly impair PFOS-induced neuronal apoptosis. These findings implicate that JNK signaling is critically involved in PFOS-induced neuronal death by virtue of mitochondrial translocation and the transcription of pro-apoptotic genes.

1. Introduction

Perfluorooctane sulfonate (PFOS) is an important component and metabolite of perfluoroorganic compounds and has been widely found in industrial productions and daily necessities, such as surface anti-fouling agents, cleaning agents, material coatings and food packaging (P. Sun et al., 2018; Wang et al., 2019). PFOS may accumulate in living organisms and is detectable in the environment, wildlife and human bodies (Fattore et al., 2018; Weber et al., 2019; Zhou et al., 2019). Animal studies have found that PFOS may cause assorted toxic effects, such as hepatotoxicity, immunotoxicity, cardiovascular toxicity, reproductive toxicity and neurotoxicity (Chen et al., 2016; Cui et al., 2015; Harada et al., 2005; Salgado et al., 2016; Yang et al., 2002), and is considered to be an environmental pollutant with multi-organic toxicity. Particularly, the neurotoxic effects of PFOS have attracted significant public health concern. Animal studies implicate that PFOS exposure is associated with spatial learning and memory impairment and multiple behavioral alterations (Spulber et al., 2014; Wang et al., 2015; Zeng et al., 2019). However, the molecular mechanism underlying PFOS neurotoxicity remains to be elucidated.

Recent studies indicated that PFOS exposure may trigger direct neuronal damage and death. In this regard, mitochondrial dysfunction and reactive oxidative species (ROS) production are supposed to play integral roles in PFOS-induced neuronal apoptosis. HG Lee et al. reported that PFOS trigger ROS-mediated PKC pathway to promote the apoptosis of cerebellar granule cells (Lee et al., 2012). Furthermore, PFOS may alter mitochondria-residual Bcl-2 proteins of hippocampal neurons in adult mice (Long et al., 2013). Another study showed that PFOS can cause neuronal apoptosis in a ROS-dependent manner (C. Li et al., 2017). However, the detailed mechanism by which PFOS may cause neuronal damage remains to be fully clarified.

JNK signaling pathway is an important stress-responsive signaling pathway, and can be activated by various external factors, including growth factors, cytokines and environmental stress (Tanaka et al., 2019). In somatic cells, robust JNK activation is frequently related with the decision of cell destiny. JNK may activate c-Jun, c-myc and other pro-survival proteins to drive cell growth under growth factor stimulation. However, numerous studies indicated that JNK play a pivotal role in the initiation of cell apoptosis following exposure to cytotoxic agents. JNK is required for UV and γ-ray-induced apoptosis

* Corresponding author.
E-mail address: jiang_shengyang@163.com (S. Jiang).

https://doi.org/10.1016/j.ntt.2019.106821
Received 28 April 2019; Received in revised form 29 July 2019; Accepted 7 August 2019
Available online 08 August 2019
0892-0362/

(Dhanasekaran and Reddy, 2008). JNK may physically bind to and phosphorylate pro-apoptotic Bcl-2 member Bim to trigger Bax-dependent apoptosis. JNK may also induce the cleavage of bid, leading to its translocation into mitochondrial membrane and resultant release of cytochrome c*(cyto c)* (Madesh et al., 2002). In addition, evidence indicates that activated JNK may translocate into mitochondria to directly trigger mitochondria-dependent apoptotic signaling (Kharbanda et al., 2000). These findings suggest a crucial involvement of JNK signaling in the determination of cell survival and apoptosis.

Our recent findings have implicated that PFOS may trigger neuronal apoptosis via ROS and mitochondria-dependent manners. In the present study, we showed that PFOS exposure robustly activated JNK signaling in SH-SY5Y cells with a concomitant increase of neuronal apoptosis. Notably, active JNK exhibits significant mitochondrial and nuclear translocation following PFOS exposure. Treatment with ROS scavenger NAC impairs PFOS-initiated mitochondrial and nuclear translocation of phosphorylated JNK (p-JNK). In addition, abrogating JNK activity or scavenging ROS partially attenuates PFOS-induced neuronal apoptosis. These findings suggest a critical involvement of ROS-mediated JNK signaling in PFOS-mediated neuronal death, shedding new light into the mechanism underlying PFOS-induced neurological disorders.

2. Materials and methods

2.1. Reagents

The following reagents were purchased from their suppliers: PFOS (potassium salt, purity 98%; Sigma-Aldrich, Shanghai, China); Dimethyl Sulfoxide (DMSO; Sigma, St. Louis, MO, USA); *N*-acetyl cysteine (NAC; Sigma, St. Louis, MO, USA); SP600125 (Sigma-Aldrich Shanghai, China); MitoTracker® Red CMXRos (Yisheng Biological Technology Co Ltd., Shanghai, China).

2.2. Cell cultures and treatment

SH-SY5Y cells were obtained from the Institute of Biochemistry and Cell Biology and cultured in Dulbecco's modified Eagle's medium (DMEM; Sigma, St. Louis, MO, USA) supplemented with 10% fetal bovine serum (Sigma, St. Louis, MO, USA) at 37 °C in a humidified atmosphere with 5% CO_2. SH-SY5Y cells were exposed to different concentrations of PFOS (0, 25, 50, 100 and 200 μM) dissolved in DMSO for 48 h or 200 μM PFOS for 0, 3, 6, 12, 24 and 48 h for time-dependent experiments in the period of logarithmic phase. 0.1% DMSO was used as a vehicle control. As for NAC and SP600125 treatments, the cells were pre-treated with 10 mM ROS inhibitor (NAC) for 24 h or 10 mM SP600125 for 1 h, followed by PFOS treatment for 48 h.

2.3. Western blot analysis

SHSY-5Y cells were directly lysed using RIPA lysis buffer (Beyotime biotechnology, Shanghai) on ice for 30 min, transferred into 1.5 mL Eppendorf tubes and centrifugated at 13,000*g*, 4 °C for 10 min. The supernatants were transferred into new Eppendorf tubes and protein concentrations were determined using a BCA protein assay kit (Beyotime biotechnology). Subsequently, the samples were added with SDS sample buffer and boiled for 15 min. Equal protein samples were separated by sodium dodecyl sulfate-polyacrylamide gel electrophoresis (SDS-PAGE) and transferred to PVDF membranes. Next, PVDF membranes were blocked with 5% skim milk in TBST for 2 h. The membranes were incubated with the indicated primary antibodies overnight at 4 °C and secondary antibodies at room temperature for 2 h. Finally, the protein bands were visualized using an enhanced chemiluminescence system (ECL, Thermo Scientific Pierce, Rockford, IL).

2.4. Annexin-V/7-AAD analysis of SH-SY5Y cell apoptosis

Annexin-V/7-AAD analysis was performed using an Annexin-V/7-AAD apoptotic assay kit (BD Pharmingen, USA) in accordance with the manufacturer's instruction. After treatments, cells were trypsinized and washed twice with ice-cold PBS. Thereafter, the cells were resuspended with 100 μL of 1 × binding buffer. Each tube was added with 5 μL Annexin V-FITC and 5 μL 7-AAD, mixed gently, and incubated for 15 min in dark at room temperature. Finally, the samples were added with 400 μL of 1× Binding Buffer and subjected to flow cytometry analysis shortly afterwards.

2.5. ROS measurements

SH-SY5Y cells were seeded in 6-well plate (1.2×10^6 cells per well), incubated overnight and exposed to DMSO (control), 50, 100 and 200 μM PFOS for 48 h. The medium of the cells were removed and replaced with fresh serum-free medium containing DCFH-DA (1:1000; Sigma, St. Louis, MO, USA). After 30 min incubation at 37 °C, Hoechst-33258 (1:1000; Santa Cruz Biotechnology) was added to stain cell nuclei. The fluorescent signal was examined under a fluorescence microscope (Leica Microsystems GmbH, Wetzlar, Germany). The experiments were repeated in triplicate.

2.6. Cell fluorescence analysis

SH-SY5Y cells were incubated with MitoTracker® Red CMXRos (Yisheng Biological Technology Co Ltd., Shanghai, China) in culture medium at 37 °C for 30 min in dark. Then, the cells were fixed with 4% (*v*/v) paraformaldehyde in PBS for 50 min and permeabilized with 1% Triton-X100 for 15 min. The cells were blocked with a blocking buffer containing 1% (w/v) bovine serum albumin (BSA) and 0.05% Tween-20 in PBS for 2 h at room temperature and incubated with a rabbit polyclonal anti-p-JNK antibody (1:100, Santa Cruz Biotechnology) overnight at 4 °C. Thereafter, the cells were incubated with an Alexa Fluor® 488-conjucated secondary antibody (Life Technologies, Shanghai, China) and Hoechst-33258 for 2 h at room temperature. Finally, fluorescent images were captured using a digital fluorescence microscope (DM5000, Leica Microsystems GmbH, Wetzlar, Germany).

2.7. Mitochondria, nuclear and cytoplasm extraction

SH-SY5Y cells were treated with or without 200 μM PFOS for 48 h, in the presence or absence of pretreatment with NAC, SP600125. Subsequently, mitochondrial and cytoplasmic fractions of SH-SY5Y cells were isolated using a mitochondria isolation kit (Beyotime Institute of Biotechnology, Jiangsu, China) following the manufacturer's recommended protocol. Subcellular fractionation was performed using a Nuclear and Cytoplasmic Protein Extraction Kit (Sangon Biotech Shanghai Co Ltd).

2.8. Statistical analysis

All data are presented as the means ± standard deviation of the mean (SD) from at least three independent experiments. Statistical significant difference was calculated by one-way analysis of variance (ANOVA). Statistical comparisons were made between two groups using Student's *t*-test. The differences were considered statistically significant when $P < 0.05$.

3. Results

3.1. JNK signaling pathway was activated in PFOS-treatment cells

To decipher the role of JNK signaling in PFOS-induced neuronal apoptosis, we first analyzed the activity of JNK signaling in PFOS-

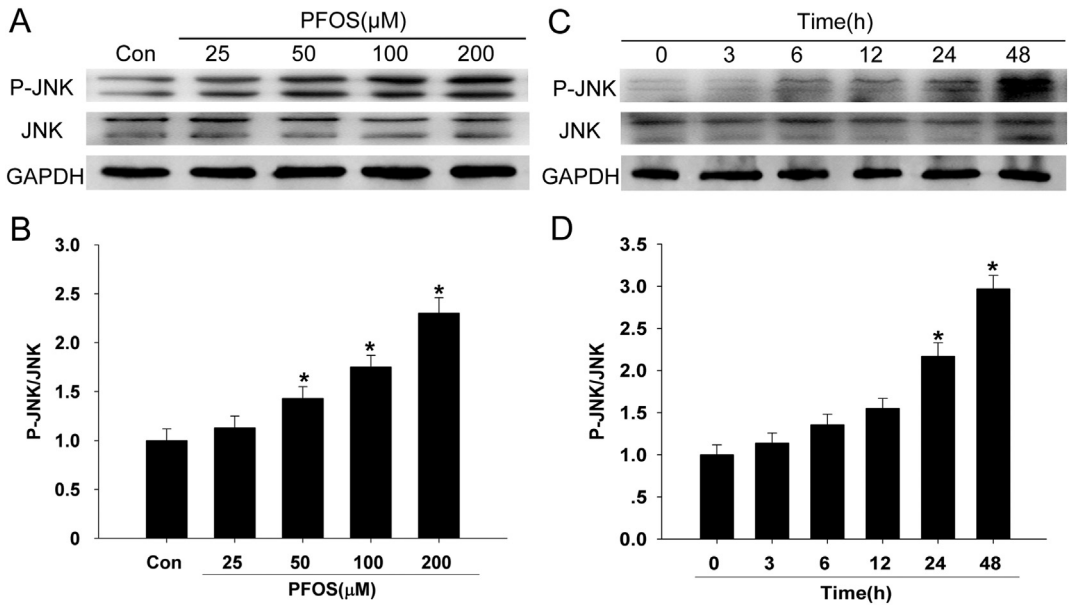

Fig. 1. PFOS induces JNK phosphorylation in dose- and time-dependent manners. (A) SH-SY5Y cells were exposed to different doses of PFOS (0, 25, 50, 100 and 200 μM) for 48 h and subjected to western blot analysis using the indicated antibodies. (B) Quantitative analysis of the ratio of p-JNK/JNK. (C) SH-SY5Y cells were exposed to 200 μM PFOS for different time periods (0, 3, 6, 12, 24 and 48 h). Representative Western blots for phospho-JNK, JNK and GAPDH in SH-SY5Y cells. (D) The chart showed quantitative results of the ratio of p-JNK/JNK. Values are mean ± SEM ($n = 3$). * $P < 0.05$, compared with the control group.

exposed SH-SY5Y cells. Cells were exposed to different concentrations of PFOS for 48 h. It was found that the level of phosphorylated JNK (p-JNK) increased in response to PFOS concentration while the total amount of JNK protein remained largely unchanged, suggesting that JNK signaling pathway was robustly activated following PFOS exposure (Fig. 1A and B). In addition, the phosphorylation of JNK also exhibited a time-dependent increase, reaching a maximum at 48 h in PFOS-exposed SH-SY5Y cells (Fig. 1C and D). These findings suggest that PFOS induced the activation of JNK signaling in dose- and time-dependent manners.

3.2. PFOS triggers neuronal apoptosis at a dose range comparable to that initiating JNK signaling

To determine whether PFOS-induced JNK signaling is relevant to neuronal apoptosis, Annexin V/7-AAD (AV/7-AAD) apoptotic assay was conducted. In the early stages of apoptosis, membranal phosphatidylserine (PS) normally distributed on the cytoplasmic side of the lipid bilayer of the cell membrane is translocated into the outer side of the plasma membrane. Annexin V may specifically probe PS molecules that undergo translocation in apoptotic cells. PFOS exposure led to the apoptosis of SH-SY5Y cells at a starting dose of 50 μM, and the level of apoptosis increased in a dose-dependent manner (Fig. 2A). The histograms are statistical data for Annexin V positive cells and represent the total number of early and late apoptotic cells (Fig. 2B). These results indicate that the apoptosis of SH-SY5Y cells is exacerbated following exposed to increased concentrations of PFOS.

3.3. Altered expression of apoptosis-related molecules in PFOS-exposed SH-SY5Y cells

Apoptosis refers to the programmed death of cells under precise physiological or pathological conditions, which are precisely regulated by multiple genes (Bouton et al., 2004). Among the many apoptosis-regulating genes, Bcl-2 proteins are indispensible regulators of mitochondrial apoptotic pathway (Zhao et al., 2013). Bcl-2 and Bax are representative members of Bcl-2 family and play pivotal roles in the regulation of apoptosis (Zhang et al., 2012). Bcl-2 has anti-apoptotic effect while Bax has pro-apoptotic effect, and caspase 3 is a late-stage executor of apoptosis (Choudhary et al., 2015). The results showed that the expression of Bax and cleaved caspase 3 increased after PFOS exposure (Fig. 3A), while the protein expression of anti-apoptotic protein Bcl-2 declined compared with the control group. This indicates that PFOS promotes the activation of apoptosis-related molecules and promotes the occurrence of apoptosis in a dose-dependent manner (Fig. 3B).

3.4. PFOS induces ROS accumulation in a dose-dependent manner

Since ROS plays an important role in PFOS-induced neuronal apoptosis (Dong et al., 2015), we tested the production of ROS in SH-SY5Y cells under different concentrations of PFOS. Reactive oxygen species were detected using the fluorescent probe DCFH-DA, and the non-fluorescent DCFH-DA was hydrolyzed into DCFH by the esterase when it entered the cell, the intracellular ROS can oxidize the non-fluorescent DCFH to fluorescent DCH. As shown in Fig. 4, ROS production was increased in PFOS-stimulated cells in a dose-dependent manner compared with the control group, which was consistent with previous studies, indicating that PFOS can cause an increase in ROS and potentially cause adverse damage to cells.

3.5. p-JNK is accumulated both in the mitochondria and the nucleus after PFOS exposure

To clarify the detailed distribution of activated JNK in PFOS-exposed neurons, SH-SY5Y cells were labeled with p-JNK, Mito Tracker (mitochrondrial marker) and Hoechst-33258. We found that p-JNK was lowly detected in SH-SY5Y cells in the control group, and was robustly upregulated following PFOS exposure, whereas pretreatment with NAC and SP600125 can alleviate the activation of JNK (Fig. 5A). Importantly, cytoplasmic p-JNK had colocalization with MitoTracker, suggesting that cytoplasmic p-JNK might be distributed in mitochondria (Fig. 5A). To further determine the expression pattern of p-JNK in cells, we probed the level of p-JNK in nuclear and mitochondrial fractions. As shown in Fig. 5B and C, the level of p-JNK in nuclear and mitochondrial fractions was dramatically elevated following PFOS

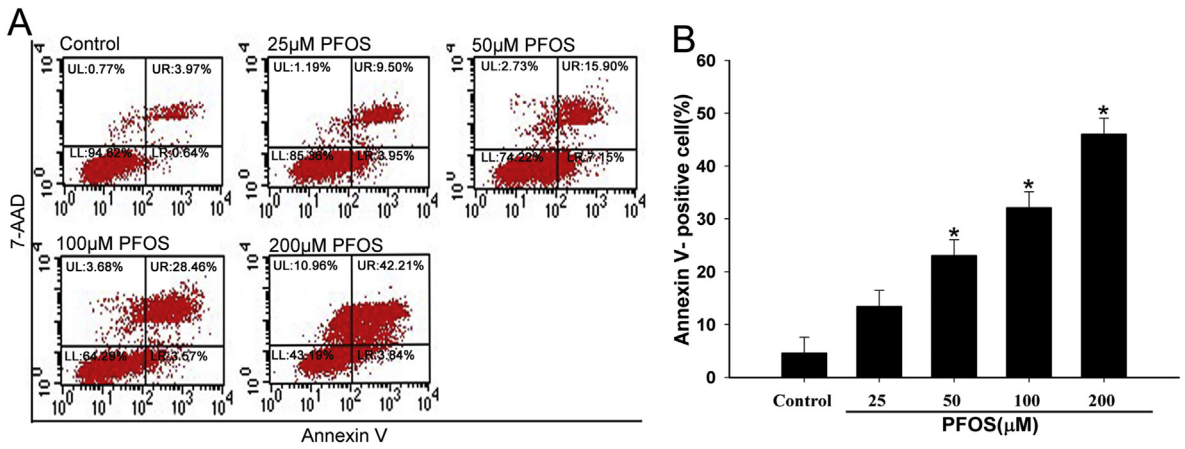

Fig. 2. PFOS induces the apoptosis of SH-SY5Y cells. (A) SH-SY5Y cells were exposed to different concentrations of PFOS (0, 25, 50, 100 and 200 μM) for 48 h. Cell apoptosis was determined using flow cytometry analysis. LL: viable cells, LR: early-apoptotic cells, UR: late-apoptotic cells, UL: mechanically broken cells. (B) The histogram represents the proportion of Annexin-V positive cells in the indicating groups. The experiments were repeated at least three times. Data are shown as mean ± SD (n = 3). * P < 0.05, compared with the control group.

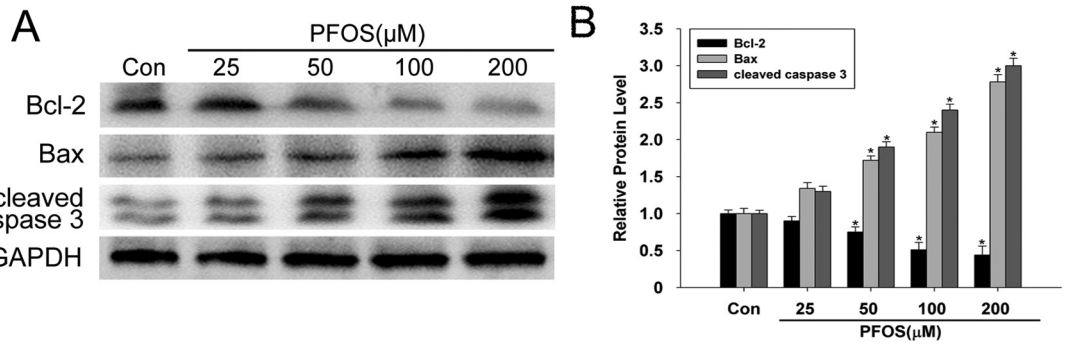

Fig. 3. Altered expression of apoptosis-related proteins following PFOS exposure. (A) SH-SY5Y cells were exposed to different doses of PFOS (0, 25, 50, 100 and 200 μM) for 48 h. The levels of Bcl-2, Bax and cleaved caspase 3 were determined using Western blot analysis. (B) The histogram denoted the density ratios of Bcl-2, Bax and cleaved caspase 3 to GAPDH. Values are mean ± SEM (n = 3). * P < 0.05, compared with the control group.

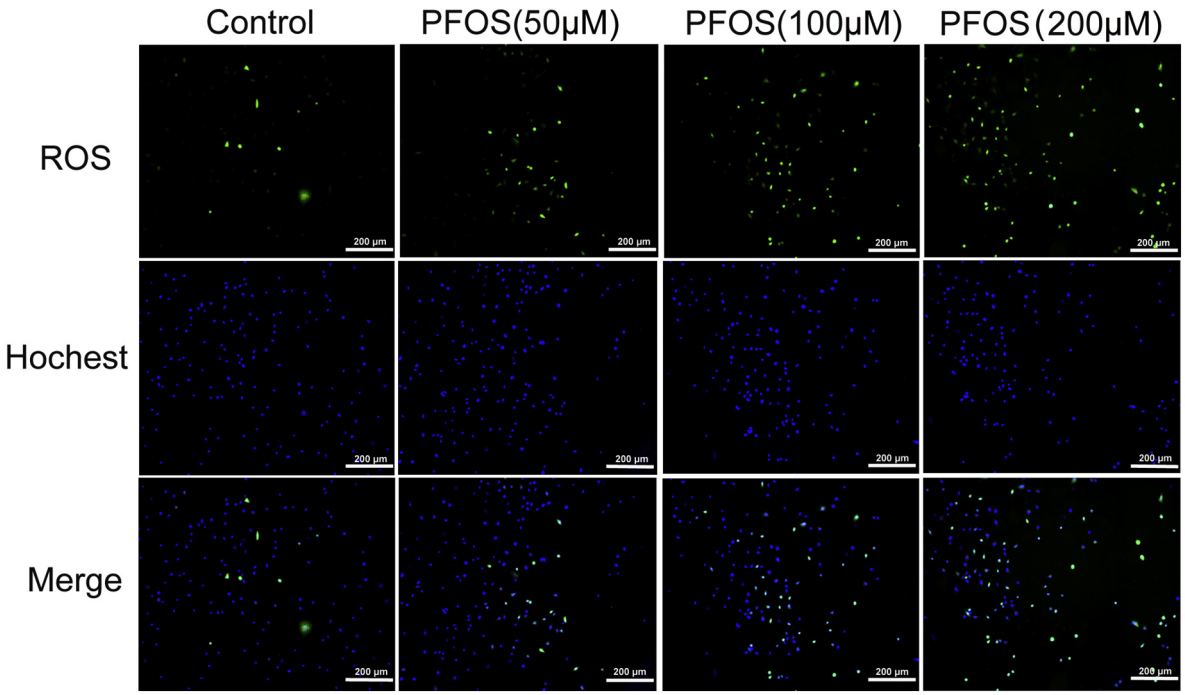

Fig. 4. PFOS induces ROS production in a dose-dependent manner. SH-SY5Y cells were exposed to 0, 50, 100 and 200 μM PFOS for 48 h. Intracellular ROS were detected using ROS fluorescence probe DCFH-DA under a digital fluorescence microscope. Scale bars: 200 μm.

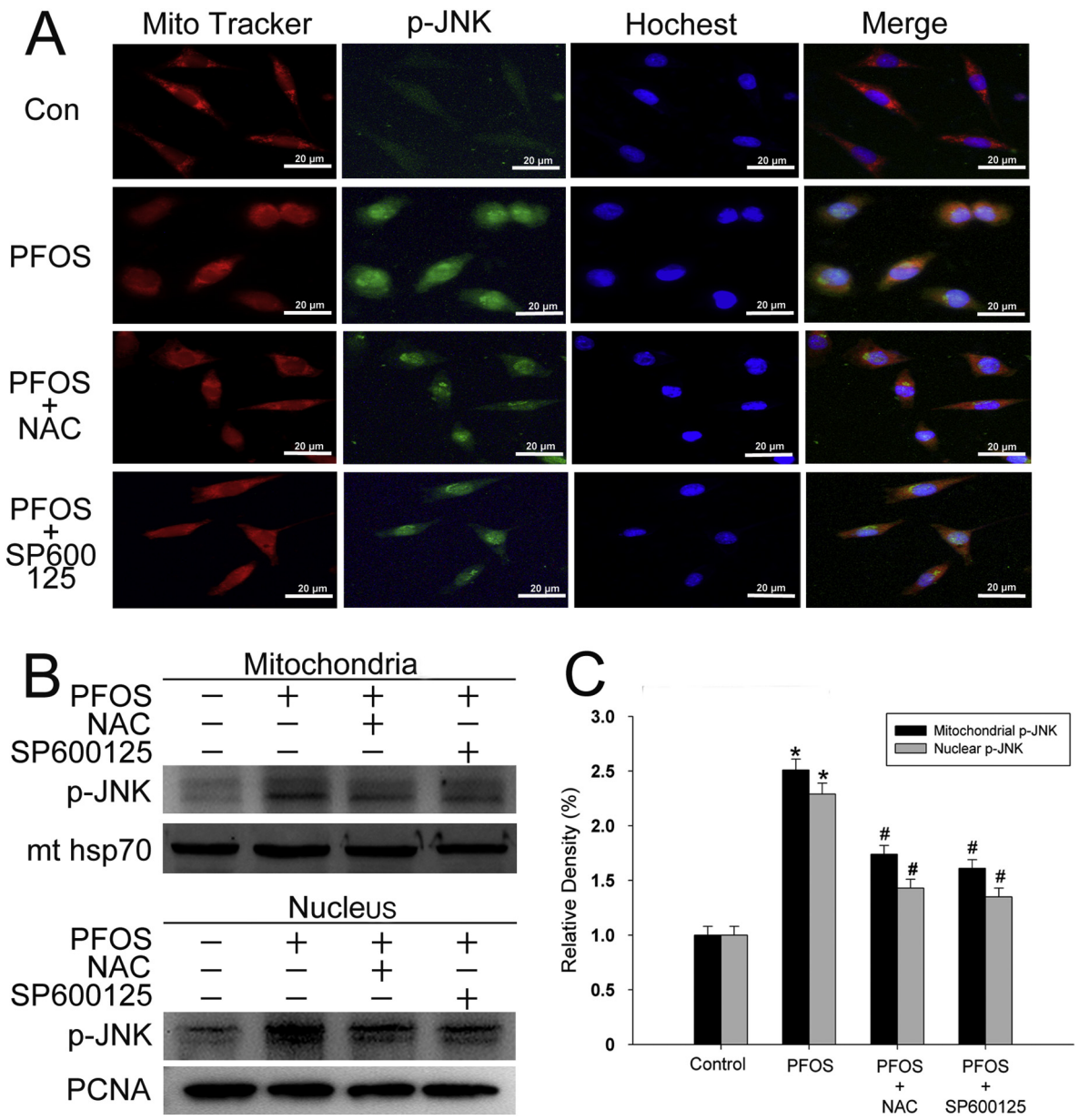

Fig. 5. JNK was activated and translocated into the mitochondria following PFOS exposure. (A) SH-SY5Y cells were treated with or without 200 μM PFOS for 48 h, and subjected to immunofluorescence analysis to determine p-JNK distribution (green). MitoTracker Red CMXRos was used to label mitochondria (red), and nuclei were counterstained with Hoechst-33258 (blue). The yellow color observed in merged images indicates p-JNK mitochondrial translocation. (B) After the indicated treatment, SH-SY5Y cells were fractioned using a mitochondria isolation kit. Next, the nuclear and mitochondrial fractions were probed for p-JNK, PCNA (nuclear marker) and mt Hsp70 (mitochondria marker) using Western blot analysis. (C) Histograms of the relative level of p-JNK to PCNA (nuclear fraction) or mt Hsp70 (mitochondrial fraction) in control and PFOS-exposed SH-SY5Y cells. Scale bars: 20 μm. Values are mean ± SEM (n = 3). * $P < 0.05$, compared with the control group; # $P < 0.05$ compared with the PFOS-only group. (For interpretation of the references to color in this figure legend, the reader is referred to the web version of this article.)

exposure and alleviated by NAC and SP600125 pretreatment. These results implicated that under PFOS exposure, JNK can translocate into mitochondria and nuclei, while pretreatment with NAC and SP600125 can alleviate the translocation of activated JNK.

3.6. JNK signaling facilitates Bim expression and mitochondrial release of cyto c in PFOS-exposed SH-SY5Y cells

Because PFOS exposure can result in nuclear and mitochondrial translocation of p-JNK, we speculated that JNK may initiate neuronal apoptosis through the expression of pro-apoptotic proteins and mitochondrial disorders. Bim is a member of the BH3-only subfamily of the Bcl-2 family and is involved in JNK-mediated apoptosis (Weber et al., 2016). We found that PFOS can trigger the expression of Bim in a dose-dependent manner using Western blot analysis (Fig. 6A), whereas pretreatment with NAC and SP600125 can impair the upregulation of Bim (Fig. 6B), indicating that ROS play an important role in JNK-mediated expression of Bim.

To further clarify the involvement of mitochondrial malfunction in PFOS-mediated apoptosis, we examined the expression of Bcl-2 and Bax in mitochondria. As shown in Fig. 6C, PFOS trigger apparent down-regulation of mitochondrial Bcl-2 and increased expression of Bax, where these effects were attenuated after the pretrentment of NAC and SP600125. Meanwhile, we analyzed the expression of cytochrome c (cyto c) in cytoplasmic and mitochondrial fractions. As predicted, PFOS exposure induced marked release of cyto c from the mitochondria to the

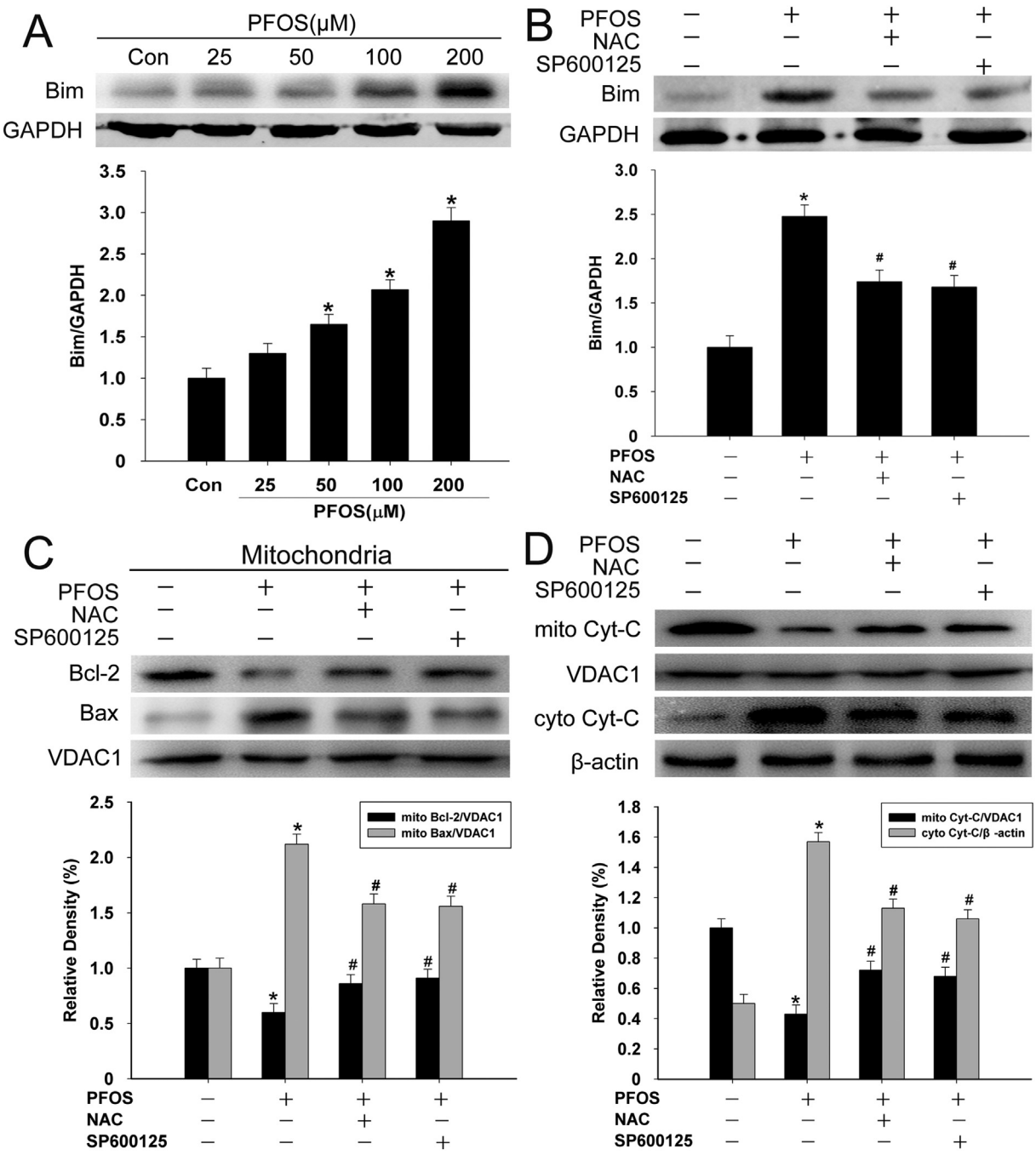

Fig. 6. PFOS exposure triggers expression changes of Bcl-2 proteins and mitochondrial cyto c into the cytosol through ROS- and JNK-dependent mechanisms. (A) SH-SY5Y cells were exposed to different concentrations of PFOS (0, 25, 50, 100 and 200 μM) for 48 h and subjected to Bim detection using Western blot analysis. The histogram denoted the density ratio of Bim to GAPDH. (B) SH-SY5Y cells were pretreated with or without NAC (10 mM) for 24 h or SP600125 (10 mM) for 1 h and then exposed to 200 μM PFOS. Western blot analysis was conducted to determine Bim protein in DMSO or PFOS-exposed cells. The histogram denoted the density ratio of Bim to GAPDH. (C) SH-SY5Y cells received the indicated treatments and were subjected to fractionation assay using a mitochondria isolation kit. Next, the mitochondrial fractions were probed for Bcl-2, Bax and VDAC1 (mitochondria marker) expression using Western blot analysis. The histogram indicated the density ratios of Bcl-2 and Bax to VDAC1. (D) The protein level of cyto c was detected using Western blot analysis in the mitochondria (mito) and cytoplasm (cyto). The histogram denoted the density ratios of mitochondrial cyto c to VDAC1 and cytoplasm cyto c to β-actin. Values are mean ± SEM (n = 3). * $P < 0.05$, compared with the control group; # $P < 0.05$, compared with the PFOS-only group.

cytoplasm, whose effects was diminished by the treatment with NAC and SP600125 (Fig. 6D). These results further demonstrate that ROS and JNK contribute to PFOS-induced apoptosis through altering the expression apoptosis-related proteins and the initiation of mitochondrial cyto c release.

3.7. Roles of ROS and JNK signaling pathway in PFOS-induced apoptosis

Finally, we examined the role of oxidative stress and the JNK signaling pathway in PFOS-induced apoptosis. Firstly, western blot analysis revealed that PFOS triggered the expression of cleaved caspase 3 in NAC- and JNK-dependent manners (Fig. 7A and B). Next, Annexin-V/7-AAD assay was performed to validate the role of ROS and JNK signaling

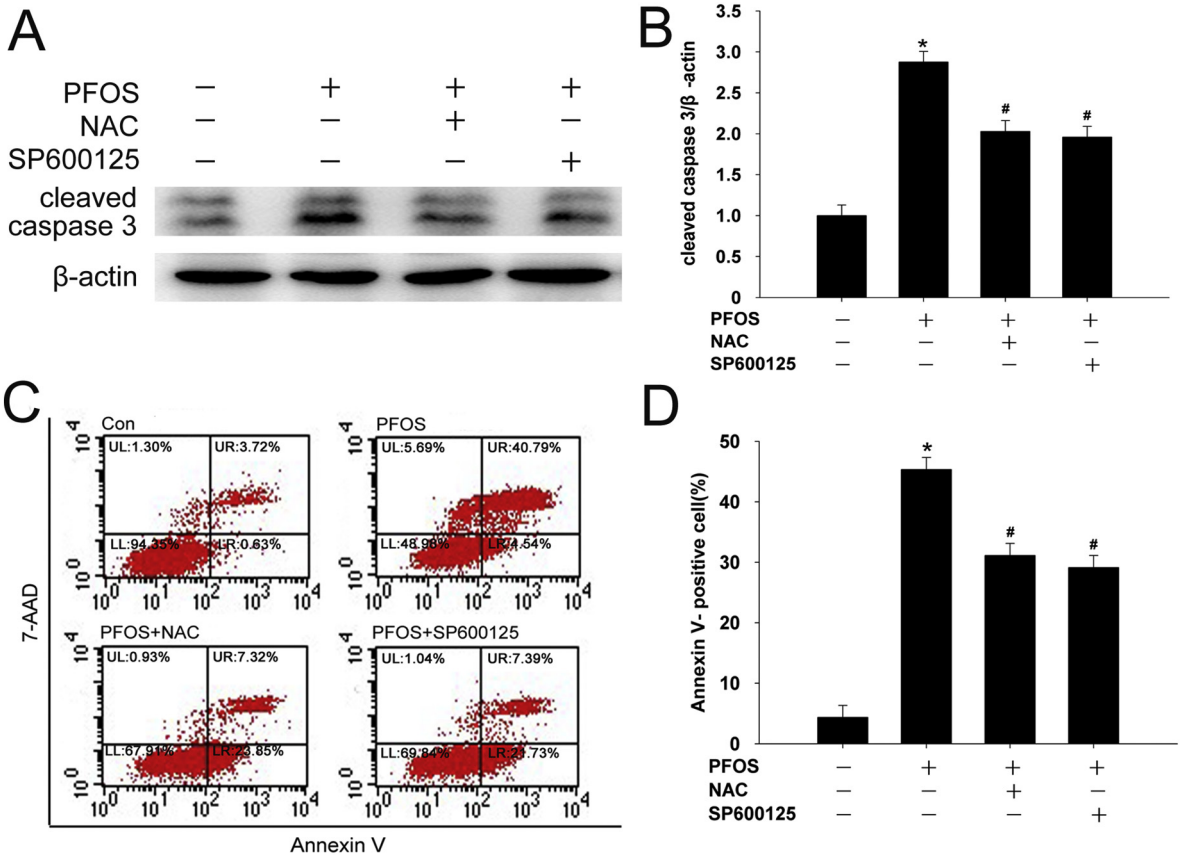

Fig. 7. ROS and JNK signaling play important roles in PFOS-induced apoptosis. SH-SY5Y cells were pretreated with or without NAC (10 mM) for 24 h or SP600125 (10 mM) for 1 h and then exposed to 200 μM PFOS. (A) Western blot analysis of cleaved caspase 3 protein in SH-SY5Y cells. (B) The histogram showed the density ratio of cleaved caspase 3 to β-actin. (C) Cell apoptosis was determined using flow cytometry analysis in the indicated groups. (D) The histogram represents the proportion of Annexin-V positive cells. Values are mean ± SEM (n = 3). * P < 0.05, compared with the control group; # P < 0.05 (compared with the PFOS-only group).

in PFOS-mediated neuronal apoptosis. As shown in Fig. 7C and D, NAC and SP600125 can significantly reduce the apoptosis of SH-SY5Y cells induced by PFOS, from 45.33% ± 2.05% to 31.12% ± 1.57% or 29.12% ± 1.75%, respectively. This suggests that reducing ROS production and blocking JNK signaling pathway can effectively alleviate PFOS-induced apoptosis.

4. Discussion

Neurotoxicology represents an important aspect of the adverse effects of PFOS on mammals, as multiple investigations revealed apparent neurological and behavioral disorders following chronic PFOS exposure (Dusza et al., 2018; Khezri et al., 2017). Some reports indicate that PFOS may cause direct neuronal damage and consequent neuronal apoptosis (Guo et al., 2017). However, the molecular mechanisms by which PFOS triggers neuronal death remain largely obscure. In the present study, we revealed that JNK signaling plays a crucial role in PFOS-induced neuronal apoptosis. PFOS exposure leads to rapid mitochondrial and nuclear translocation of JNK, resulting in the expression of pro-apoptotic proteins and the initiation of mitochondrial apoptotic pathway. The activation of JNK pathway is attributed to ROS accumulation in PFOS-exposed cells. Antagonizing JNK activity or scavenging ROS markedly impaired PFOS-induced expression of pro-apoptotic proteins and neuronal apoptosis. These findings together implicate that ROS accumulation and JNK activation may critically contribute to PFOS-induced neuronal apoptosis, shedding new light on the molecular mechanisms underlying PFOS neurotoxicology (Fig. 8).

Serving as a critical stress-responsive pathway, JNK signaling is

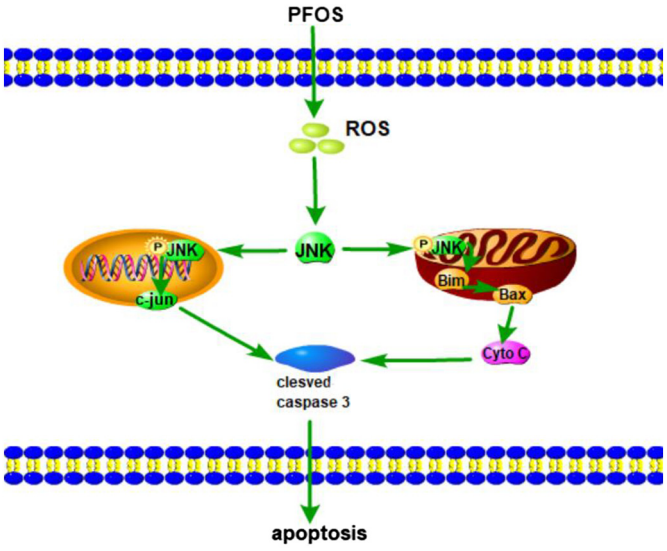

Fig. 8. Schematic diagram of the roles of ROS and JNK in PFOS-initiated neuronal apoptosis.

frequently activated following unfavorable external stimuli, and consequently plays a determinant role in the decision of cell fate. Aberrant JNK activation has been widely regarded as an important driver of cell apoptosis, though some studies also suggested a pro-survival role of JNK in some cell types (Wu et al., 2019). JNK is essential for cell

apoptosis induced by UV radiation and genotoxic agents (Jia et al., 2018). JNK plays an integral role in extrinsic apoptotic pathways as well as mitochondrial-dependent intrinsic apoptotic pathways. Indeed, studies have indicated that PFOS may initiate p53 signaling to promote the apoptosis of somatic cells in mice, and JNK may potentially contribute to this process (Dong et al., 2012). Our recent work also found that Nrf2, other substrate of JNK, is involved in PFOS-induced neuronal apoptosis, implicating a complicated role of JNK in PFOS-induced neuronal death (P. Sun et al., 2018). Our present study suggests that JNK may also promote the expression of pro-apoptotic Bcl-2 proteins to trigger mitochondrial apoptotic cascades. In addition to Bcl-2 members, JNK may also translocate into the nucleus to phosphorylate transcription factors and facilitate apoptosis. Multiple studies have indicated that JNK/c-JUN signaling may initiate neuronal apoptosis through the transcription of pro-apoptotic proteins, including Bim and PUMA (Akhter et al., 2015; Tan et al., 2013). Furthermore, FOXO proteins, especially FOXO1 and FOXO3a, are also documented to participate in JNK-triggered neuronal apoptosis (Li et al., 2015; Weng et al., 2016). Moreover, JNK may exert its pro-apoptotic function through direct mitochondrial translocation and this is an indicative event suggesting the involvement of JNK in apoptosis. The translocation of JNK, along with Bim and Bax, from the cytoplasm into the mitochondria increases mitochondrial outer membrane permeability transition, thereby promoting the release of cyto c from the mitochondria into the cytoplasm, triggering a caspase 8/caspase 3 apoptotic cascade (Yu et al., 2019). In line with this notion, our experiments demonstrate that blockade of JNK pathway have a significant effect on PFOS-induced cyto c release. All of these findings implicate that PFOS-induced JNK activation may provoke neuronal apoptosis through multiple mechanisms.

ROS have been regarded as crucial players in neuronal death under various pathological conditions. ROS may initiate multiple signaling pathways, such as p53-p21, JNK and FOXO pathways, to trigger neuronal death (Johnson et al., 2019). In addition, various studies indicated that ROS are direct executors of cell death (Polyak et al., 1997; Simon et al., 2000). ROS may directly promote mitochondrial permeability and the release of cyto c to initiate apoptosis (Zhang et al., 2019). ROS have been documented to play indispensible roles in neuronal apoptosis, as eliminating ROS accumulation protected neurons from mitochondrial dysfunction and death induced by a various stress stimuli (R. Li et al., 2017; Y. Sun, et al., 2018). Notably, ROS production is regulated by various pro-apoptotic pathways. In this regard, JNK has been proposed as an important signaling to exacerbate ROS production during apoptotic program. Chambers JW and LoGrasso PV reported that mitochondrial JNK promoted superoxide production and the amplification of mitochondrial ROS through modulating Complex I activity during stress (Chambers and LoGrasso, 2011). Thus, we speculate that mitochondrial translocation of JNK may play a role in ROS accumulation and consequent ROS-mediated neuronal damage and death. Further studies are required to clarify this hypothesis.

5. Conclusions

In summary, we reported the neurotoxic mechanism of PFOS may involve ROS-mediated JNK activation and mitochondrial translocation preceding neuronal apoptosis. The activation of JNK may cause neuronal apoptosis through its action on mitochondria-dependent pathway. Treatment with ROS scavenger NAC or JNK inhibitor SP600126 can effectively alleviate PFOS-induced JNK activation and neuronal apoptosis. The findings together infer that JNK signaling is an important effecter of PFOS-induced neuronal death, implicating that targeting JNK pathway may protect neurons from PFOS-induced apoptosis.

Declaration competing interest

There is no conflict of interest.

Transparency document

The transparency document associated with this article can be found, in online version.

Acknowledgments

This work was supported by the National Natural Science Foundation of China (81573188) and Science and Technology Project of Nantong (MS12017015-4, YYZ17031).

References

Akhter, R., Sanphui, P., Das, H., Saha, P., Biswas, S.C., 2015. The regulation of p53 up-regulated modulator of apoptosis by JNK/c-Jun pathway in beta-amyloid-induced neuron death. J. Neurochem. 134 (6), 1091–1103.
Bouton, L.A., Ramirez, C.D., Bailey, D.P., Yeatman, C.F., Yue, J., Wright, H.V., Domen, J., Rosato, R.R., Grant, S., Fischer-Stenger, K., Ryan, J.J., 2004. Costimulation with interleukin-4 and interleukin-10 induces mast cell apoptosis and cell-cycle arrest: the role of p53 and the mitochondrion. Exp. Hematol. 32 (12), 1137–1145.
Chambers, J.W., LoGrasso, P.V., 2011. Mitochondrial c-Jun N-terminal kinase (JNK) signaling initiates physiological changes resulting in amplification of reactive oxygen species generation. J. Biol. Chem. 286 (18), 16052–16062.
Chen, J., Wang, X., Ge, X., Wang, D., Wang, T., Zhang, L., Tanguay, R.L., Simonich, M., Huang, C., Dong, Q., 2016. Chronic perfluorooctanesulphonic acid (PFOS) exposure produces estrogenic effects in zebrafish. Environmental pollution (Barking, Essex : 1987) 218, 702–708.
Choudhary, G.S., Al-Harbi, S., Almasan, A., 2015. Caspase-3 activation is a critical determinant of genotoxic stress-induced apoptosis. Methods in molecular biology (Clifton, N.J.) 1219, 1–9.
Cui, Y., Liu, W., Xie, W., Yu, W., Wang, C., Chen, H., 2015. Investigation of the effects of perfluorooctanoic acid (PFOA) and perfluorooctane sulfonate (PFOS) on apoptosis and cell cycle in a zebrafish (Danio rerio) liver cell line. Int. J. Environ. Res. Public Health 12 (12), 15673–15682.
Dhanasekaran, D.N., Reddy, E.P., 2008. JNK signaling in apoptosis. Oncogene 27 (48), 6245–6251.
Dong, G.H., Wang, J., Zhang, Y.H., Liu, M.M., Wang, D., Zheng, L., Jin, Y.H., 2012. Induction of p53-mediated apoptosis in splenocytes and thymocytes of C57BL/6 mice exposed to perfluorooctane sulfonate (PFOS). Toxicol. Appl. Pharmacol. 264 (2), 292–299.
Dong, L., Yang, X., Gu, W., Zhao, K., Ge, H., Zhou, J., Bai, X., 2015. Connexin 43 mediates PFOS-induced apoptosis in astrocytes. Chemosphere 132, 8–16.
Dusza, H.M., Cenijn, P.H., Kamstra, J.H., Westerink, R.H.S., Leonards, P.E.G., Hamers, T., 2018. Effects of environmental pollutants on calcium release and uptake by rat cortical microsomes. Neurotoxicology 69, 266–277.
Fattore, E., Bagnati, R., Colombo, A., Fanelli, R., Miniero, R., Brambilla, G., Di Domenico, A., Roncarati, A., Davoli, E., 2018. Perfluorooctane sulfonate (PFOS), perfluorooctanoic acid (PFOA), brominated dioxins (PBDDs) and furans (PBDFs) in wild and farmed organisms at different trophic levels in the Mediterranean Sea. Toxics 6 (3).
Guo, X.X., He, Q.Z., Li, W., Long, D.X., Pan, X.Y., Chen, C., Zeng, H.C., 2017. Brain-derived neurotrophic factor mediated perfluorooctane sulfonate induced-neurotoxicity via epigenetics regulation in SK-N-SH cells. Int. J. Mol. Sci. 18 (4).
Harada, K., Xu, F., Ono, K., Iijima, T., Koizumi, A., 2005. Effects of PFOS and PFOA on L-type Ca2+ currents in guinea-pig ventricular myocytes. Biochem. Biophys. Res. Commun. 329 (2), 487–494.
Jia, Y., Qin, Q., Fang, C.P., Shen, W., Sun, T.T., Huang, Y.L., Li, W.J., Deng, A.M., 2018. UVB induces apoptosis via downregulation of CALML3-dependent JNK1/2 and ERK1/2 pathways in cataract. Int. J. Mol. Med. 41 (5), 3041–3050.
Johnson, S.C., Pan, A., Li, L., Sedensky, M., Morgan, P., 2019. Neurotoxicity of anesthetics: mechanisms and meaning from mouse intervention studies. Neurotoxicol. Teratol. 71, 22–31.
Kharbanda, S., Saxena, S., Yoshida, K., Pandey, P., Kaneki, M., Wang, Q., Cheng, K., Chen, Y.N., Campbell, A., Sudha, T., Yuan, Z.M., Narula, J., Weichselbaum, R., Nalin, C., Kufe, D., 2000. Translocation of SAPK/JNK to mitochondria and interaction with Bcl-x(L) in response to DNA damage. J. Biol. Chem. 275 (1), 322–327.
Khezri, A., Fraser, T.W., Nourizadeh-Lillabadi, R., Kamstra, J.H., Berg, V., Zimmer, K.E., Ropstad, E., 2017. A mixture of persistent organic pollutants and perfluorooctanesulfonic acid induces similar behavioural responses, but different gene expression profiles in zebrafish larvae. Int. J. Mol. Sci. 18 (2).
Lee, H.G., Lee, Y.J., Yang, J.H., 2012. Perfluorooctane sulfonate induces apoptosis of cerebellar granule cells via a ROS-dependent protein kinase C signaling pathway. Neurotoxicology 33 (3), 314–320.
Li, D., Li, X., Wu, J., Li, J., Zhang, L., Xiong, T., Tang, J., Qu, Y., Mu, D., 2015. Involvement of the JNK/FOXO3a/Bim pathway in neuronal apoptosis after hypoxic-ischemic brain damage in neonatal rats. PLoS One 10 (7), e0132998.
Li, C., Liu, X., Liu, Q., Li, S., Li, Y., Hu, H., Shao, J., 2017. Protection of taurine against PFOS-induced neurotoxicity in PC12 cells. Adv. Exp. Med. Biol. 975 (Pt 2), 907–916.
Li, R., Zhou, P., Guo, Y., Lee, J.S., Zhou, B., 2017. Tris (1, 3-dichloro-2-propyl) phosphate induces apoptosis and autophagy in SH-SY5Y cells: involvement of ROS-mediated AMPK/mTOR/ULK1 pathways. Food and chemical toxicology : an international journal published for the British Industrial Biological Research Association 100,

183–196.
Long, Y., Wang, Y., Ji, G., Yan, L., Hu, F., Gu, A., 2013. Neurotoxicity of perfluorooctane sulfonate to hippocampal cells in adult mice. PLoS One 8 (1), e54176.
Madesh, M., Antonsson, B., Srinivasula, S.M., Alnemri, E.S., Hajnoczky, G., 2002. Rapid kinetics of tBid-induced cytochrome c and Smac/DIABLO release and mitochondrial depolarization. J. Biol. Chem. 277 (7), 5651–5659.
Polyak, K., Xia, Y., Zweier, J.L., Kinzler, K.W., Vogelstein, B., 1997. A model for p53-induced apoptosis. Nature 389 (6648), 300–305.
Salgado, R., Lopez-Doval, S., Pereiro, N., Lafuente, A., 2016. Perfluorooctane sulfonate (PFOS) exposure could modify the dopaminergic system in several limbic brain regions. Toxicol. Lett. 240 (1), 226–235.
Simon, H.U., Haj-Yehia, A., Levi-Schaffer, F., 2000. Role of reactive oxygen species (ROS) in apoptosis induction. Apoptosis : an international journal on programmed cell death 5 (5), 415–418.
Spulber, S., Kilian, P., Wan Ibrahim, W.N., Onishchenko, N., Ulhaq, M., Norrgren, L., Negri, S., Di Tuccio, M., Ceccatelli, S., 2014. PFOS induces behavioral alterations, including spontaneous hyperactivity that is corrected by dexamfetamine in zebrafish larvae. PLoS One 9 (4), e94227.
Sun, P., Nie, X., Chen, X., Yin, L., Luo, J., Sun, L., Wan, C., Jiang, S., 2018. Nrf2 signaling elicits a neuroprotective role against PFOS-mediated oxidative damage and apoptosis. Neurochem. Res. 43 (12), 2446–2459.
Sun, Y., Sukumaran, P., Selvaraj, S., Cilz, N.I., Schaar, A., Lei, S., Singh, B.B., 2018. TRPM2 promotes neurotoxin MPP(+)/MPTP-induced cell death. Mol. Neurobiol. 55 (1), 409–420.
Tan, M., Li, Z., Ma, S., Luo, J., Xu, S., Lu, A., Gan, W., Su, P., Lin, H., Li, S., Lai, B., 2013. Heroin activates Bim via c-Jun N-terminal kinase/c-Jun pathway to mediate neuronal apoptosis. Neuroscience 233, 1–8.
Tanaka, K.I., Shimoda, M., Kasai, M., Ikeda, M., Ishima, Y., Kawahara, M., 2019. Involvement of SAPK/JNK signaling pathway in copper enhanced zinc-induced neuronal cell death. Toxicological sciences : an official journal of the Society of Toxicology 169 (1), 293–302.
Wang, Y., Liu, W., Zhang, Q., Zhao, H., Quan, X., 2015. Effects of developmental perfluorooctane sulfonate exposure on spatial learning and memory ability of rats and mechanism associated with synaptic plasticity. Food and chemical toxicology : an international journal published for the British Industrial Biological Research Association 76, 70–76.
Wang, R., Wang, R., Niu, X., Cheng, Y., Shang, X., Li, Y., Li, S., Liu, X., Shao, J., 2019. Role of astrocytes-derived d-serine in PFOS-induced neurotoxicity through NMDARs in the rat primary hippocampal neurons. Toxicology 422, 14–24.
Weber, A., Heinlein, M., Dengjel, J., Alber, C., Singh, P.K., Hacker, G., 2016. The deubiquitinase Usp27x stabilizes the BH3-only protein Bim and enhances apoptosis. EMBO Rep. 17 (5), 724–738.
Weber, R., Bell, L., Watson, A., Petrlik, J., Paun, M.C., Vijgen, J., 2019. Assessment of pops contaminated sites and the need for stringent soil standards for food safety for the protection of human health. Environmental pollution (Barking, Essex : 1987) 249, 703–715.
Weng, Q., Liu, Z., Li, B., Liu, K., Wu, W., Liu, H., 2016. Oxidative stress induces mouse follicular granulosa cells apoptosis via JNK/FoxO1 pathway. PLoS One 11 (12), e0167869.
Wu, Q., Wu, W., Fu, B., Shi, L., Wang, X., Kuca, K., 2019. JNK signaling in cancer cell survival. Med. Res. Rev. 47 (1), 2670–2677.
Yang, Q., Abedi-Valugerdi, M., Xie, Y., Zhao, X.Y., Moller, G., Nelson, B.D., DePierre, J.W., 2002. Potent suppression of the adaptive immune response in mice upon dietary exposure to the potent peroxisome proliferator, perfluorooctanoic acid. Int. Immunopharmacol. 2 (2–3), 389–397.
Yu, X., Yu, R.Q., Zhang, X., Zhan, F., Sun, X., Wu, Y., 2019. DDT exposure induces cell cycle arrest and apoptosis of skin fibroblasts from Indo-Pacific humpback dolphin via mitochondria dysfunction. Aquatic toxicology (Amsterdam, Netherlands) 213, 105229.
Zeng, Z., Song, B., Xiao, R., Zeng, G., Gong, J., Chen, M., Xu, P., Zhang, P., Shen, M., Yi, H., 2019. Assessing the human health risks of perfluorooctane sulfonate by in vivo and in vitro studies. Environ. Int. 126, 598–610.
Zhang, L., Jia, L., Cui, S., Shi, Y., Chang, A., Wang, P., Zhang, Z., 2012. AP-2alpha-dependent regulation of Bcl-2/Bax expression affects apoptosis in the trophoblast. J. Mol. Histol. 43 (6), 681–689.
Zhang, Y., Wang, X., Chen, C., An, J., Shang, Y., Li, H., Xia, H., Yu, J., Wang, C., Liu, Y., Guo, S., 2019. Regulation of TBBPA-induced oxidative stress on mitochondrial apoptosis in L02cells through the Nrf2 signaling pathway. Chemosphere 226, 463–471.
Zhao, J., Wu, J.X., Yang, W., 2013. Expression of caspase-3, Bcl-2, and Bax in pentavalent vanadium-induced neuronal apoptosis. Zhonghua lao dong wei sheng zhi ye bing za zhi = Zhonghua laodong weisheng zhiyebing zazhi = Chinese journal of industrial hygiene and occupational diseases 31 (8), 589–592.
Zhou, W., Zhao, S., Tong, C., Chen, L., Yu, X., Yuan, T., Aimuzi, R., Luo, F., Tian, Y., Zhang, J., 2019. Dietary intake, drinking water ingestion and plasma perfluoroalkyl substances concentration in reproductive aged Chinese women. Environ. Int. 127, 487–494.